Density Matrix Renormalization Group study of ^{48}Cr and ^{56}Ni

B. Thakur† S. Pittel† and N.Sandulescu‡
† *Bartol Research Institute and Department of Physics and Astronomy, University of Delaware, Newark, DE 19716, USA and*
‡ *Institute of Physics and Nuclear Engineering, 76900, Bucharest, Romania*
(Dated: February 9, 2009)

We discuss the development of an angular-momentum-conserving variant of the Density Matrix Renormalization Group (DMRG) method for use in large-scale shell-model calculations of atomic nuclei and report a first application of the method to the ground state of ^{56}Ni and improved results for ^{48}Cr. In both cases, we see a high level of agreement with the exact results. A comparison of the two shows a dramatic reduction in the fraction of the space required to achieve accuracy as the size of the problem grows.

PACS numbers: 21.60.Cs, 05.10.Cc

One of the foremost challenges confronting nuclear physics today is the systematic study of medium-mass and heavy nuclei using the shell model. Even with the drastic truncation achieved by limiting the active particles to one or at most a couple of valence shells outside a doubly magic core, the size of the resulting space still exceeds storage capabilities of the currently available computational resources for all but fairly light nuclei. This opens up the need for innovative truncation strategies. The Density Matrix Renormalization Group (DMRG) method has had outstanding success dealing with low-dimensional quantum lattice problems [1]. The method was later extended to finite fermi systems, where it has been applied with impressive success to the description of small metallic grains [2], to two-dimensional electrons in strong magnetic fields [3], and to problems in quantum chemistry [4]. This suggests that it might also prove useful in the description of another finite fermi system, the atomic nucleus. In this work we present our first results for ^{56}Ni, the most ambitious test we have considered to date, and confirm its usefulness for nuclear structure calculations.

The usual DMRG algorithm begins by partitioning the complete Hilbert space for a given problem onto a set of lattice sites, with each site admitting a set of basis states. The untruncated problem is recovered by considering the complete set of states within all sites. Since the full space is typically too large for exact treatment, the DMRG method treats the problem iteratively, by successively adding sites to those already treated and implementing a truncation based on density matrix considerations. This is illustrated schematically if Figure 1.

Assume that there are n sites on the lattice and that r sites to the left have already been treated, defining what we call the system block B_r. Assume further that within this block we have m states and the matrix elements of all suboperators of the hamiltonian for these states. The next step would be to enlarge B_r by adding the $r+1^{st}$ site, producing the enlarged block $B_{r+1} \equiv B_r \otimes L_{r+1}$. We then couple this to a medium, which involves information

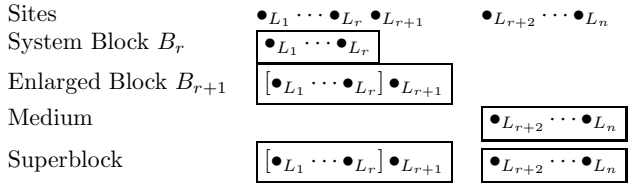

FIG. 1: Schematic illustration of the DMRG growth procedure. Shown are all the sites in the lattice chain, those of the system block, those added in the enlargement process, those of the medium, and their organization in the superblock.

on all of the remaining sites, producing the Superblock $B_r \otimes L_{r+1} \otimes M$, representing the entire system. The basic idea of the DMRG method is to truncate the enlarged block to its optimum m states, namely those that are the most significant contributors to the Superblock ground state, and to renormalize all operators to act in this truncated space.

We will assume for now a product space description and denote the states of the enlarged block as $|I\rangle_{B_{r+1}} = |i\rangle_{B_r}|j\rangle_{r+1}$, where i span the states of the system block and j those of the added site. The Superblock ground state can then be written as

$$|\Psi_g\rangle_{SB} = \sum_{I,\ k} B_{I,\ k}|I\rangle_{B_{r+1}}|k\rangle_M \ , \tag{1}$$

where k spans the states of the medium (M).

The reduced density matrix for the enlarged block in the Superblock ground state is obtained by contracting over the states of the medium, namely

$$\rho_{I,\ I'} = \sum_k B^*_{I,\ k} B_{I',\ k} \ . \tag{2}$$

If we diagonalize this reduced density matrix and maintain the eigenstates associated with its m largest eigenvalues we are guaranteed to have found the m most important components of the enlarged block in the Superblock ground state.

The basic idea then is to systematically grow the system block by adding lattice sites and then at each stage to truncate to the m most important states obtained in this way. At each stage we must, as just noted, transform all hamiltonian suboperators to the $m-$dimensional truncated space, as this provides required information for its subsequent enlargement. The enlargement process just described is repeated over and over, sweeping in both directions through the set of lattice sites until convergence in the ground-state energy is obtained. The calculations can then be redone as a function of m until acceptably small changes with increasing values are obtained.

The usual DMRG procedure, as just outlined, works with product states and is thus equivalent to an m-scheme approach in the nuclear context. This has the drawback that conserving angular momentum symmetry becomes difficult. To avoid this problem in applications to nuclei, Dukelsky and Pittel [5] proposed the use of an angular-momentum-preserving variant of the DMRG, called the JDMRG. This method, which is an example of a non-Abelian DMRG algorithm [6], was first applied to nuclei in the context of the Gamow Shell Model [7] and then subsequently applied to the traditional nuclear shell model by Pittel and Sandulescu [8].

In the JDMRG, we work in a coupled (or J-scheme) basis. As a consequence, we must now calculate reduced matrix elements of the various suboperators of the Hamiltonian, namely

$$a_i^\dagger, (a_i^\dagger a_j^\dagger)^\lambda, (a_i^\dagger \tilde{a}_j)^\lambda, [(a_i^\dagger a_j^\dagger)^\lambda \tilde{a}_k]^\kappa,$$
$$[(a_i^\dagger a_j^\dagger)^\lambda (\tilde{a}_k \tilde{a}_l)^\lambda]^0 + h.c.$$

An important feature of nuclei is that they contain two types of particles, neutrons and protons. This leads to the question of how the associated orbitals should be arranged on the lattice, intertwined or at opposite ends. We have found it useful to maintain a separation between the neutron and proton blocks, leading to what we call a three-block JDMRG algorithm, for reasons to be made clear a bit later.

The nuclei for which we will present results here are ^{48}Cr and ^{56}Ni. In both we assume a doubly magic ^{40}Ca core with the remaining nucleons distributed over the orbitals of the $2p-1f$ shell. We now spell out in a bit more detail the steps of the JDMRG procedure that were implemented in our treatment of these two nuclei.

Setting the order of orbits:

As just noted, we have chosen to define the lattice chain such that the neutron and the proton orbits lie on its opposite ends. This still leaves several possible options, however. We have found the optimal order to be the one shown in Figure 2, where we use the notation n_j and p_j to denote a neutron orbital with angular momentum j and a proton orbital with angular momentum j, respectively.

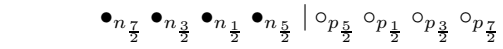

FIG. 2: The order of orbits used in the calculations described in the text.

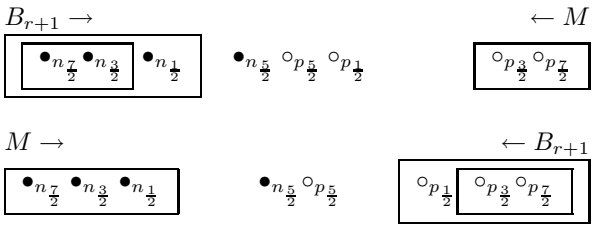

FIG. 3: Two consecutive enlargement steps during the warmup phase of the DMRG calculations described in the text. In the first, the third neutron orbit from the left is added; in the next, the third neutron orbit from the right is subsequently added.

This order places maximally entangled orbits next to one another, as is found to be important from quantum information considerations [9].

Warmup Phase(The first enlargement stage):

This phase of the DMRG procedure is aimed at defining a good initial set of states to use in each block. In our calculations, we follow the procedure schematically illustrated in Figure 3, whereby we begin by adding two orbits at one end of the chain of sites, followed by a subsequent enlargement at the other end, followed by gradual further enlargements from the two ends of the chain. In this initialization phase, the last truncated block on the opposite end of the chain is used as the medium. As should be clear, the Superblock so obtained does not contain all of the orbits. Hence the Superblock must be diagonalized for all relevant neutron and proton numbers in the $J = 0^+$ space, to permit some particles to reside in orbits not included. A mixed density matrix is constructed from the corresponding eigenstates which is then used to truncate the system to the m most important states for each block of orbits. This process is repeated until the middle of the chain, at which point all neutron and proton orbits have been treated.

At this point we have an initial choice for the m most important states for each relevant block.

The Sweep Phase(Successive enlargement stages):

We now wish to iteratively update information on each block, by gradually sweeping through the orbits and using information initially from the warmup stage and later from the previous sweep stage to define the medium. We start the sweep phase by adding the orbits from the center of the chain towards the end. The medium now consists of one of the like-particle blocks (M_1) - constructed either during the warmup or the previous sweep, and the

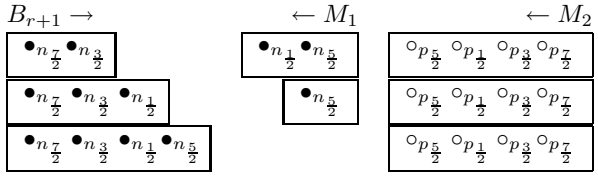

FIG. 4: Three consecutive steps in the enlargement of the neutron block from the left during the sweep phase.

unlike-particle block (M_2). The fact that our medium contains two components is why we refer to this as the three-block algorithm. The complete growth of the neutron and proton blocks is repeated in both directions until convergence is attained. Several consecutive steps in the neutron block enlargement during a given sweep stage are illustrated schematically in Figure 4. Because of the great care taken in the warmup initialization, only three to four sweeps are typically needed for the process to converge.

Convergence with m:

The above steps are repeated with increasing m until satisfactory convergence in the ground-state energy is obtained.

We present here test results for ^{48}Cr and ^{56}Ni, using the three block algorithm described above. We have used the KB3 matrix elements [10] used in Refs. [11, 12], with the same set of single-particle energies used there as well. Excited states for ^{56}Ni were not included in the analysis since they are not available for the hamiltonian that we used.

TABLE I: Calculated ground-state energies in MeV as a function of m for ^{48}Cr. The maximum dimension encountered in the sweep process is also given.

m	E_{GS}	$Max\ Dim$
40	-32.698	1,985
60	-32.763	2,859
80	-32.788	3,765
100	-32.817	4,494
120	-32.840	6,367
140	-32.890	8,217
160	-32.902	9,978
180	-32.944	11,062
200	-32.947	12,076
Exact	-32.953	41,355

The results for the ground-state energy of ^{48}Cr are shown in Table I. The full shell-model space of ^{48}Cr consists of 1,963,461 states of which 41,355 have $J^\pi = 0^+$.

The exact result for the ground state is -32.953 MeV. Though the JDMRG results converge monotonically with m to this value, we need a substantial portion (about 25%) of the full space to achieve agreement to within a few keV of the exact energy.

It should be noted that the results reported in Ref. [8] were for a different order of single-particle levels, explaining why the ground-state energies and maximum dimensions listed in that paper are different from those reported here for the same values of m.

TABLE II: Calculated energies in MeV for low-lying excited states in ^{48}Cr, with dimensions shown in brackets.

m	$E_{2_1^+}$ (Dim)	$E_{4_1^+}$ (Dim)	$E_{6_1^+}$ (Dim)	$E_{0_2^+}$ (Dim)
100	-31.98 (21,003)	-30.90 (33,261)	-29.16 (38,652)	-27.97 (44,94)
120	-32.01 (28,677)	-30.93 (42,234)	-29.20 (45,054)	-28.06 (6,367)
140	-32.04 (36,706)	-30.98 (52,254)	-29.26 (52,950)	-28.15 (8,217)
160	-32.10 (44,618)	-31.04 (63,487)	-29.34 (63,537)	-28.29 (9,978)
180	-32.13 (50,030)	-31.09 (72,616)	-29.43 (74,346)	-28.47 (11,062)
200	-32.13 (54,891)	-31.10 (81,249)	-29.47 (85,168)	-28.48 (12,076)
Exact	-32.15 (182,421)	-31.13 (246,979)	-29.55 (226,259)	-28.56 (41,355)

The results for low-lying excited states are provided in Table 2. To obtain these results, we construct the relevant hamiltonian matrices using the optimum block structures obtained at the point of the lowest ground state energy. Note that we do not target the excited states themselves in constructing the reduced density matrix used for the truncation. As a result, the convergence is not as rapid as for the ground state, but nevertheless quite acceptable.

TABLE III: Calculated ground-state energies in MeV as a function of m for ^{56}Ni. The maximum dimensions encountered in the sweep process are also given.

m	E_{GS}	$Max\ Dim$
80	-78.351	72,023
100	-78.363	83,773
120	-78.372	102,690
140	-78.376	119,797
160	-78.390	136,073
180	-78.393	162,019
200	-78.399	192,878
Exact	-78.46	15,443,684

The results for ^{56}Ni ground state are tabulated in Table

3. The size of the exact space in an angular momentum basis is 15,443,684. We have carried out these calculations with the same order of single-particle orbits as for ^{48}Cr. The fraction of space required for meaningful convergence is dramatically reduced for ^{56}Ni compared to ^{48}Cr. With about 1% of the space we are able to get within around 60 keV of the exact results [12].

Earlier calculations for ^{56}Ni using the DMRG by Papenbrock and Dean [13], although done in the m-scheme, were unable to obtain the ground state energy to better than 400 keV.

An interesting feature of our results for both ^{48}Cr and ^{56}Ni is the absence of an exponential falloff in the converged ground state energy as a function of the number of states retained. Since exponential behavior is often used to extrapolate to the actual ground state energy, it is worth commenting on why it does not occur here.

A key difference between our JDMRG algorithm and the usual DMRG is that our lattice sites vary significantly in size, as they represent complete single-particle orbits. Often, when an orbit is added, no truncation is required at that step. When the increment in m reaches a large enough value that truncation is avoided, we find a sharp drop in the ground state energy for that m value. For lower values, truncation always arises at that step in the sweep and the falloff is less severe. As a result, the energy tends to fall off in spurts as a function of m rather than as a smooth exponential, with larger orbits producing a more jagged behavior. If, however, we carry out our calculations for a wide enough range of m values, a fit can still be carried out in the presence of such behavior. Later, we discuss another way of enhancing exponential falloff in the JDMRG.

In this work, we have described our efforts aimed at developing the DMRG method as a dynamical truncation strategy for large scale shell model calculations of atomic nuclei. Following a brief description of the usual DMRG procedure, we discussed a specific three-block angular-momentum-conserving algorithm for carrying out such calculations. We presented results for two nuclei ^{48}Cr and ^{56}Ni. Although a large fraction of the space was required to achieve results of high accuracy for ^{48}Cr, the fraction of the space required for ^{56}Ni was much smaller. This bodes well for the future usefulness of the method for even larger problems.

There are several issues that we plan to explore in the near future. On the one hand, we would like to extend our test analysis to a broader range of nuclei, to more meaningfully explore the requisite fraction of the space required for convergence. We also plan to redo our calculations for ^{56}Ni to use the GXPF1A interaction [14], for which exact results are available not only for the ground state but for the states in the first deformed band as well [15]. This will help us to better assess the ability of the method to accurately treat excited states as well, even when only the ground state is being targeted in the iterative truncation process.

Finally, to be able to study even heavier nuclei, it will be necessary to include orbits with even larger angular momenta. For example, in nuclei beyond ^{56}Ni the $1g_{9/2}$ orbit becomes increasingly more important. The larger the orbit the greater is the computational strain it imposes on the iterative growth process of the DMRG. A possible way to get around this is to split such orbits into two or more parts, while still maintaining exact angular momentum conservation throughout. We plan to test some possible approaches for splitting such orbits in the context of the smaller $1f_{7/2}$ orbital and to compare the results that emerge with those we have already obtained. Hopefully this will enable us to then turn to even larger orbits and to continue our applications up in nuclear mass. Use of smaller lattice sites may also facilitate a more rapid transition to exponential behavior in the ground state energy.

This work was supported by US National Science Foundation under grant # PHY 0553127. We are grateful for the resources provided to us by the National Energy Research Scientific Computing Center. We acknowledge with deep appreciation the important contributions of Jorge Dukelsky to this project. We also wish to thank Alfredo Poves for providing the KB3 matrix elements used in this work.

[1] S. R. White, Phys. Rev. Lett. **69**, 2863 (1992).
[2] J. Dukelsky and G. Sierra, Phys. Rev. B **61**, 12302 (2000).
[3] N. Shibata and D. Yoshioka, Phys. Rev. Lett. **86**, 5755 (2001).
[4] S. R. White and R. L. Martin, J. Chem. Phy **110**, 4127 (1999).
[5] J. Dukelsky and S. Pittel, Rep. Prog. Phy **67**, 513 (2004).
[6] I. McCulloch and M. Gulácsi, Europhys. Lett. **57**, 852 (2002).
[7] N. Michel, W. Nazarewicz, M. Ploszajczak and J. Rotureau, Rev. Mex. Fisica **50** 74(2004); J. Rotureau, N. Michel, W. Nazarewicz, M. Ploszajczak and J. Dukelsky Phys. Rev. Lett. **97**, 110603 (2006).
[8] S. Pittel and N. Sandulescu, Phys. Rev. C **73**, 014301 (R) (2006).
[9] Ö. Legeza and J. Sólyom, Phys. Rev. B 68, 195116 (2003).
[10] A. Poves and A. P. Zuker, Phys. Rep. **70**, 235 (1981).
[11] E. Caurier, A. P. Zuker, A. Poves, G. Martínez-Pinedo, Phys. Rev. C **5**0, 225 (1994).
[12] E. Caurier, G. Martínez-Pinedo, F. Nowacki, A. Poves, J. Retamosa and A. P. Zuker, Phys. Rev. C **5**9, 2033 (1999).
[13] T. Papenbrock and D. J. Dean, Phys. Rev. C **67**, 051303(R) (2003).
[14] M. Honma, T. Otsuka, B. A. Brown and T. Mizusaki, Eur. Phys. J. A **25** Supp. 1, 499 (2005).
[15] M. Horoi, B. A. Brown, T. Otsuka, M. Honma and T. Mizusaki, Phys. Rev. C **73**, 061305(R) (2006).